Proc. Natl. Acad. Sci. USA
Vol. 96, pp. 4645–4649, April 1999
Neurobiology

Quantization of continuous arm movements in humans with brain injury

HERMANO IGO KREBS*†, MINDY L. AISEN‡, BRUCE T. VOLPE§, AND NEVILLE HOGAN*¶

*Newman Laboratory for Biomechanics and Human Rehabilitation, Mechanical Engineering Department, and ¶Department of Brain and Cognitive Sciences, Massachusetts Institute of Technology, 77 Massachusetts Avenue, Cambridge, MA, 02139; ‡Department of Rehabilitation Research and Development, Department of Veterans Affairs, 810 Vermont Avenue NW, 122, Washington, DC; and §Department of Neurology and Neuroscience, Cornell University Medical College and Burke Medical Research Institute, 785 Mamaroneck Avenue, White Plains, NY 10605

Communicated by Robert W. Mann, Massachusetts Institute of Technology, Cambridge, MA, March 2, 1999 (received for review July 3, 1998)

ABSTRACT **Segmentation of apparently continuous movement has been reported for over a century by human movement researchers, but the existence of primitive submovements has never been proved. In 20 patients recovering from a single cerebral vascular accident (stroke), we identified the apparent submovements that composed a continuous arm motion in an unloaded task. Kinematic analysis demonstrated a submovement speed profile that was invariant across patients with different brain lesions and provided experimental verification of the detailed shape of primitive submovements. The submovement shape was unaffected by its peak speed, and to test further the invariance of shape with speed, we analyzed movement behavior in a patient with myoclonus. This patient occasionally made involuntary shock-like arm movements, which occurred near the maximum capacity of the neuromuscular system, exhibited speed profiles that were comparable to those identified in stroke patients, and were also independent of speed.**

Despite almost a century of research corroborating Woodworth's (1) proposal that continuous movement is composed of submovements, objective quantification of the form of submovements has not been forthcoming. Hence this appealing hypothesis, that primitive submovements constitute a "building block" of more complex movements, remains unproved. For example, Crossman and Goodeve (2) expanded Woodworth's model while attempting to explain Fitts' Law (3) and considered two models: a continuous-time feedback control of velocity for a linear dynamic model, and alternatively, building on Woodworth's model, an iteractive-correction submovement model. Their experiments suggested that a feedback-velocity control model could not explain the discontinuities and ripples observed in their wrist-rotation trajectories, whereas the submovement model could. Therefore, they proposed that a single displacement shape, occurring periodically and scaled appropriately, could account for complex movements. They assumed submovements with displacement vs. time in the shape of an error function (erf). Later, the periodicity aspect of Crossman & Goodeve's iteractive-correction submovement model was proven to be unacceptable (4, 5).

Nevertheless, Crossman and Goodeve's suggestion of a single submovement shape scaled and dilated to describe the continuous movement is one of the earliest suggestions that movement segments have invariant characteristics and constitute the primitives or building blocks of more complex movements. Their suggestion of an error function to describe the segment displacement was followed by others such as B-Splines, minimum jerk, minimum snap, minimum crackle, minimum time, minimum energy, and minimum acceleration (6–9).

Experimental results for point-to-point movements in two and three dimensions further support the segmentation hypothesis. For example, when Abend *et al.* (10) required subjects to draw semicircles in the horizontal plane, the hand path usually had a segmented appearance, as if the subjects were trying to approximate the semicircle by a small number of low-curvature elements. Flash and Henis (11) reported experiments on movements in two dimensions that showed how segments were blended. In their experiment, the arm trajectory modification in response to an unexpected target displacement was obtained by superimposing a new plan for moving between the first and second target onto the ongoing movement. The initial arm movement was not aborted but added to the movement resulting from the new plan. Milner (12) suggested that the iterative-correction submovement model proposed by Woodworth holds for three-dimensional movement. His experiment consisted of a series of peg-insertion tasks. Consistent with Woodworth and Crossman & Goodeve's models, for smaller hole sizes, the number of apparent submovements increased. Observing that the initial part of subjects' movement velocity profiles was highly repeatable, he proposed to identify submovement kinematics by using that data to construct a template for the acceleration phase. For the deceleration phase, he used data from the fastest movements, which had the lowest accuracy constraints and which appeared to be free of submovements. This approach constitutes an assumption that point-to-point movements with minimal accuracy requirements are executed as a single "submovement" and although this hypothesis is appealing, it remains unproven.

Similar observations have been reported in the field of child psychology and development. Von Hofsten and Lindhagen (13–15) ran a series of experiments among infant subjects 12–24 weeks old until they become "mature" babies at 36 weeks old. The task consisted of reaching for a moving multicolored "wobbler." The results suggested that movement is composed of an "initial impulse" followed by a sequence of finer adjustments (similar to Woodworth's "initial impulse and current control") and that with maturation, these submovements blended into a single segment that resembled adult movements. Lee *et al.* (6) in adults and Berthier (17) in infants used minimum-jerk velocity profiles to decompose these classes of reaching movements. A more complete overview of the submovement literature can be found elsewhere (18).

Although these and other similar experimental observations suggest that submovements are ubiquitous, proof of their existence and detailed quantification of their form have been elusive. The latter is important because if the submovement shape was known (e.g., the time profile of any measured variable such as velocity), then decomposition to extract

The publication costs of this article were defrayed in part by page charge payment. This article must therefore be hereby marked "*advertisement*" in accordance with 18 U.S.C. §1734 solely to indicate this fact.

PNAS is available online at www.pnas.org.

†To whom reprint requests should be addressed. e-mail: hikrebs@mit.edu.

submovements from a continuous-movement record would be feasible; without it, the problem is indeterminate (a "classical" example of a hard inverse problem) as any compactly supported function f(x) can be approximated with arbitrary precision in the L2-sense (mean-squared convergence) by a weighted sum of ridge functions or radial basis functions (19–21). Thus, any of an infinite set of candidate submovement shapes could fit with little objective basis to choose between them.

One way to resolve this problem would be to observe the shape of a submovement in isolation. A unique opportunity to do so arose from our ongoing work studying the feasibility of applying robotic technology to assist neurological recovery (22–24). Kinematic records of the arm movements of patients recovering from a focal brain injury (stroke) showed compelling evidence for the first time that early post-stroke recovered motions are composed of isolated segments; and that these segments become progressively more blended or overlapped as recovery proceeds. Fig. 1*A* shows an initially hemiplegic patient's first successful attempt to draw a circle. Fig. 1*A Left* shows a plan view of the patient's hand path; Fig. 1*A Right* shows the movement's speed vs. time. The speed profile has the appearance of a sequence of pulses, dropping nearly to zero between adjacent peaks, suggesting that the task (to draw a circle) is being executed as a sequence of submovements. More important, at this early stage of recovery, there is minimal overlap of submovements. As recovery continues, these disconnected submovements appear to coalesce (see Fig. 1*A Lower*). For comparison, Fig. 1*B* shows the hand path and speed profile of an unimpaired subject performing the same task. Although the circle appears to be drawn with a single continuous movement, the speed profile still suggests segmentation (although less pronounced or more overlapped).

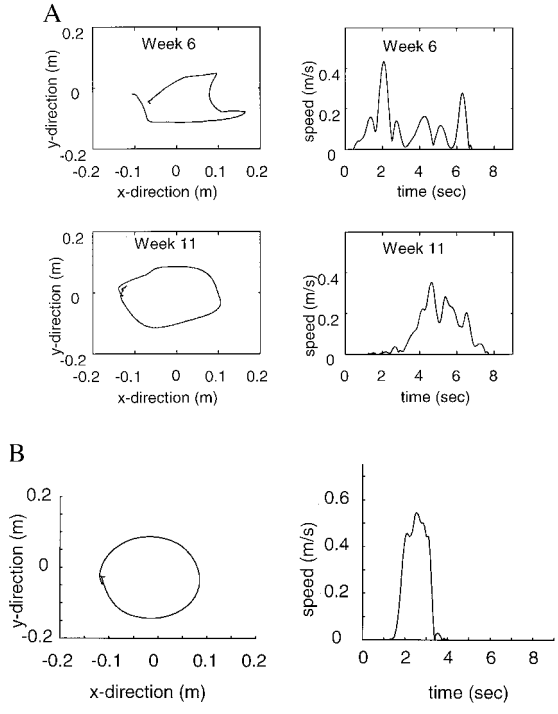

FIG. 1. (*A*) Patient A drawing clockwise single circles starting and ending at the 9:00 position. Patients wear a hand-holder that connects their palm to the robot end-effector and an elbow support. Patients were instructed to draw a smooth circle, while their hand was in view. No explicit feedback was provided. (*B*) Unimpaired subject drawing clockwise single circle starting and ending at the 9:00 position. Subject grasped the robot handle with the palm and was instructed to draw a smooth circle, while the hand was in view. No explicit feedback was provided.

Our observation of discontinuous movement behavior in recovering stroke patients prompted us to test whether the kinematic records would permit quantification of the shape of a submovement in isolation. Like prior researchers, we could not objectively isolate primitives from continuous movements made by unimpaired subjects, but movements made by stroke patients early in recovery reveal their elementary components more clearly. This affords a unique opportunity: if, as postulated, submovements are a basic feature of human motor behavior, then the "signature" shapes of submovements may be identifiable by straightforward analysis of the movements made by stroke patients early in recovery.

METHODS

We examined the speed profiles of 20 consecutive patients with acute hemiparesis caused by a single computer tomography-verified cerebral vascular accident (stroke) in the cortical or subcortical motor area (clinical details can be found in refs. 22 and 23) and of 1 patient who had action myoclonus after a cardiac arrest and global cerebral ischemia. All studies were performed with the approval of the Massachusetts Institute of Technology Committee on the Use of Humans as Experimental Subjects and the Burke Rehabilitation Hospital Human Subject Committee. Written consent was obtained from all subjects or their designated guardians.

All patients were asked to perform a visually evoked and visually guided planar unloaded task on MIT-MANUS, a robot designed for clinical neurological applications (25). They moved the robot end-effector from its initial position to a target in a simple point-to-point reaching movement. Outboard targets were at fixed positions equally spaced around a horizontal circle of 10-cm diameter and were presented in a clockwise fashion starting at the 12:00 position. The inner "home" target was presented after each of the outboard targets. Fig. 2 shows a representative raw data record of a movement of an initially hemiplegic patient during the initial stages of recovery. *Left* shows a plan view of the patient's hand path; *Right* shows the movement's speed.

Because the apparent submovements in this data appeared to vary in magnitude, duration, and time of incidence, we identified submovement kinematics based on a working hypothesis that the speed profile, s(t), of a continuous movement is composed of a finite sum of identically shaped submovements with speed profile, f( ), which may be dilated in duration, translated in time, and modulated in magnitude, i.e.,

$$s(t) = \sum_{i}^{n} m_i f\left(\frac{t - t_i}{d_i}\right),$$

where d_i, t_i, and m_i are the dilation, translation, and modulation parameters, respectively, for each submovement. The first two successful attempts to hit the target were selected for each of the 20 stroke patients enrolled in the study. To remove the

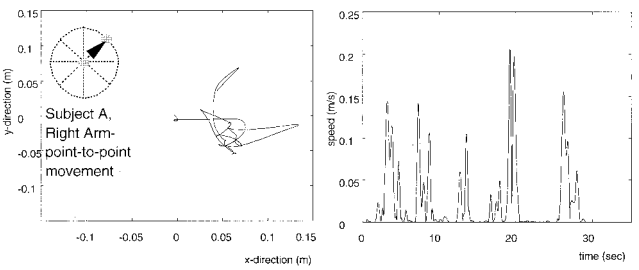

FIG. 2. Kinematic data of patient A in a point-to-point movement without time constraint. (*Left*) The hand displacement in the horizontal plane. (*Right*) Hand speed.

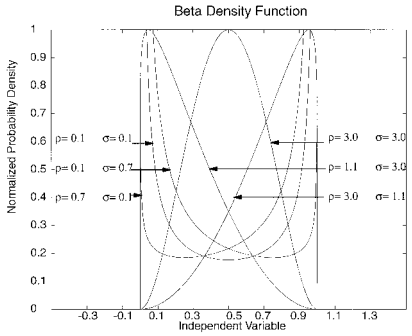

FIG. 3. Examples of normalized β-density function for different values of r and s. The figure shows that the proper choice of parameters leads to a wide variety of shapes, e.g., symmetric, skewed, unimodal, bimodal.

effects of time-translation, the complete speed record was copied and time-shifted to align all peaks above an arbitrary threshold (20% of the highest peak) to the same center. To remove the effects of magnitude modulation, the peaks were scaled to unit magnitude. Only data up to the first reversal (i.e., local minima adjacent to the local maximum that defines the peak) were retained.‖

Although the typical range of submovement durations in our data was 0.25–1 sec, some of the submovements had comparable durations, and the interpolation and decimation operations required to account for time-dilation by rescaling the time axis would have introduced unacceptable numerical errors. Instead, we chose to fit the submovement speed profile to a density function by using a standard procedure that preserved the shape and normalized the time duration to the [0, 1] interval. Specifically, for each attempt to hit the target, the data resulting from eliminating translation and modulation effects were averaged. Each of the resulting curves was fitted to a β-function by using standard techniques (26). The β-function was chosen for convenience because different values of its two parameters yield a wide variety of shapes, including symmetric, skewed, unimodal and bimodal, as illustrated in Fig. 3. Because 1 of our 20 patients did not recover any voluntary movement in any direction, this resulted in 38 β-functions, each fitted to a curve obtained from an average of 4.5 peaks (174 peaks total).

Surprisingly, we found that submovement speed profiles were remarkably similar even though neurological damage was not. Fig. 4 shows the fitted β-function mean (p) and standard deviation (ps) for all movements analyzed from all patients. The submovement speed profiles were highly stereotyped, as indicated by the consistency of the β-function mean and standard deviation ($p = 0.47 \pm 0.04$ and $ps = 0.18 \pm 0.02$). A β-function with these values is nearly symmetric and mesokurtic, with skewness = 0.07 and kurtosis = -0.62.

Fig. 4 also displays all 38 β-functions (thin dashed) along with the ensemble best-fit β-function with p = 0.47 and ps = 0.18 (solid line), graphically illustrating the consistency of the

‖Using the speed copies until the first reversal, i.e., the local minima adjacent to the local maximum that defines the peak, is an adequate approach if the speed drops to zero. Otherwise, the approach introduces a bias toward less platykurtic shapes. To check the influence of this bias, we repeated the fitting procedure using speed copies until half the time duration between the speed peak and the first reversal if that did not occur near zero (which suggested "leakage" from adjacent submovement), i.e., we continued to use the complete speed copy until the first reversal, if it occurred near zero, otherwise we used only half the time duration between the speed peak and the first reversal. The resulting new set of 38 β-functions were very similar to those observed from the original procedure. A one-way ANOVA showed that the variance, skewness, and kurtosis were not statistically different at the 0.01 level. We therefore concluded that this bias was negligible for our data.

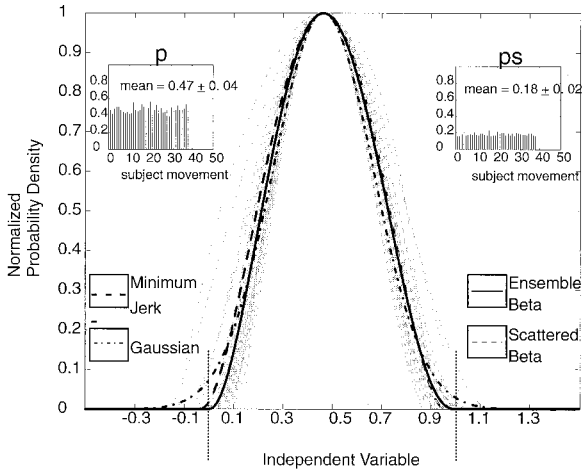

FIG. 4. Normalized β-density function parameters for the stroke patients. The *Insets* show the parameters (mean p and standard deviation ps) for the β-density function, which were estimated from the first two recorded movements for each point-to-point task from the stroke patients. The figure shows the ensemble best-fit β-function superimposed on each of the 38 individual β-functions, as well as a Gaussian with standard deviation equal to half the width of the ensemble β-function at 0.67 and a minimum-jerk curve with the same normalized displacement and duration. The peaks of all curves are centered at the same point.

submovement speed profiles. For comparison, a Gaussian profile with a standard deviation equal to half the width of the ensemble best-fit β-function at the 0.67 level and a minimum-jerk profile with the same duration are also shown, the peaks of all profiles being centered at the same location. The ensemble best-fit β-function, Gaussian, and minimum-jerk profiles are quite similar, the differences among them being smaller than the scatter of the set of β-functions. This result demonstrates that, given the variability of the data, other mathematical functions (which may be analytically more con-

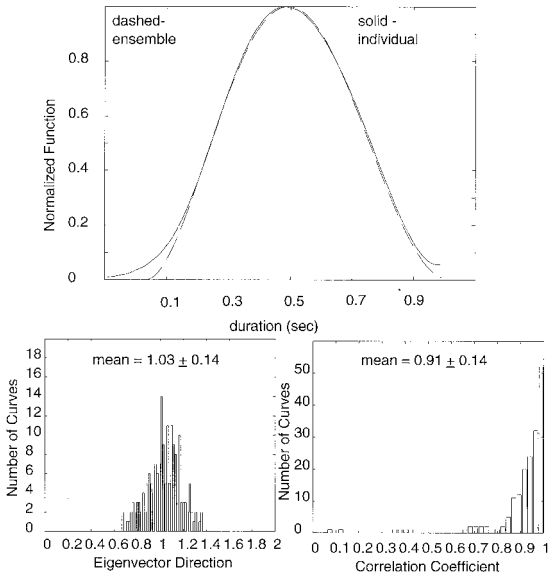

FIG. 5. Assessment of the ensemble best-fit β-function. (*Upper*) An example of an individual speed profile (solid line) compared with the ensemble best-fit β-function (dashed line). (*Lower Left*) The histogram of the slope of the principal eigenvector of the covariance matrix between the individual speed profiles and the ensemble best-fit β-function. The histogram on the *Lower Right* shows the correlation coefficient between the individual speed profiles and the ensemble best-fit β-function.

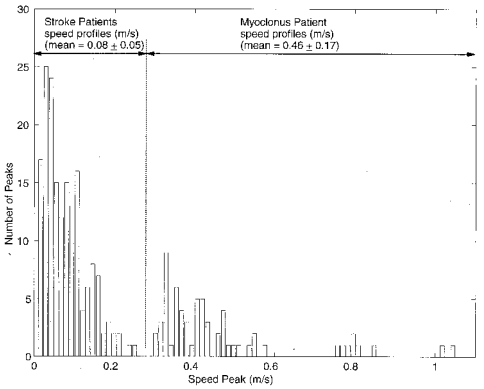

FIG. 6. Histogram of the individual speed profiles for stroke and myoclonus patients. The stroke patients' movements were typically slow (left distribution), whereas the myoclonus patient's involuntary shock-like movements were fast (right distribution), near the maximum capacity of the neuromuscular system.

venient) could describe the submovement kinematics equally well.

To assess whether our data analysis procedure properly accounted for any variation of submovement shape with duration, we compared individual submovements (all 174 speed profiles) to the ensemble best-fit β-function. Fig. 5 *Upper* compares a representative individual speed profile to the ensemble best-fit β-function. Fig. 5 *Lower Left* shows a histogram of the slopes of the principal eigenvector of the covariance matrix computed between each of the individual curves (174 speed profiles) and the ensemble best-fit β-function; this measure is centered at 1.03 with a standard deviation of 0.14. To assess whether our data analysis procedure captured the shape of the submovement, Fig. 5 *Lower Right* shows a histogram of the correlation coefficient between each speed copy and the ensemble best-fit β-function (174 speed profiles). The median correlation coefficient is 0.95, further evidence of the consistency of our data.

The experimental results summarized in Fig. 4 were obtained from stroke patients during the early stages of recovery. They had different cortical or subcortical lesions, and their movements were typically slow. A single patient with posthypoxic-action myoclonus gave us the opportunity to investigate rapid movements.** In contrast to stroke, myoclonus results in brief, involuntary shock-like movements at nearly the maximum capacity of the neuromuscular system. Fig. 6 shows the range of peak speeds observed for the myoclonus (63 speed profiles) and stroke patients (174 speed profiles). For the myoclonus patient, speed peaks above 0.3 m/sec were normalized to unit magnitude and time-shifted to align their peaks. As before, only data up to the first reversal were retained, and the resulting curves were fitted to a β-function, revealing a highly repeatable speed profile with $p = 0.52 \pm 0.04$ and $ps = 0.17 \pm 0.02$. (A β-function with these values is nearly symmetric and mesokurtic with skewness $= -0.05$ and kurtosis $= -0.56$.) This speed profile is shown in Fig. 7 along with minimum-jerk and Gaussian profiles fitted as before. Considering that the shock-like movements of the myoclonus patient were an order of magnitude faster than those of the stroke patients, so that the effects of arm inertia and muscular dynamics may distort the actual movement from that commanded by the nervous system, a direct statistical comparison between these two sets of data should be made with caution. Nevertheless, a one-way

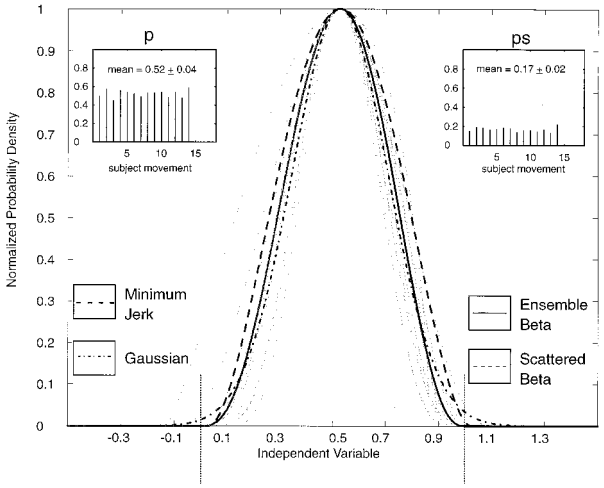

FIG. 7. Normalized β-density function parameters for the myoclonus shock-like movements. The *Insets* show the parameters (mean p and standard deviation ps) for the β-density function, which were estimated from recorded movements from the myoclonus patient during point-to-point task. The figure shows the ensemble best-fit β-function superimposed on each of the 14 individual β-functions, as well as a Gaussian with standard deviation equal to half the width of the ensemble β-function at 0.67 and a minimum-jerk curve with the same normalized displacement and duration. The peaks of all curves are centered at the same point.

ANOVA showed that the variance and kurtosis were not statistically different at the $P = 0.01$ level. The skewness was significantly different, but the speed profiles were still quite similar: the sum of the squared differences between the profiles was 0.4% of their area.

DISCUSSION

Studying the kinematics of movements made by patients with neurological injury presents a unique opportunity to capture "isolated" exemplars of submovements, presumably because the motor control processes that would normally coordinate and overlap these segments are disrupted. Our results show that the first movements made by recovering hemiplegic stroke patients were clearly segmented. Despite the wide range of peak speeds observed in those segments, they exhibited a remarkably invariant speed-vs.-time profile. This profile was also strikingly similar to that observed during the involuntary shock-like myoclonic movements of a post-cardiac arrest patient, despite an order-of-magnitude difference in their peak speeds. Indeed, taken together, the observed range of peak segment speeds for myoclonus and stroke patients covers the whole spectrum of human arm movement and supports the robustness of the finding. The remarkable invariance we observed suggests that submovements may be represented in terms of their kinematics. This would imply that they should remain invariant under different loading conditions, but our data cannot address this question as they were obtained under comparable loading conditions. Whether submovements reflect some sort of kinematic strategy or stereotypic neural activation pattern or neuromuscular force command remains to be determined. Nevertheless, the identified speed profile was remarkably similar to that observed when unimpaired human subjects made simple point-to-point unconstrained reaching movements in the horizontal or vertical plane at different speeds and also at different handheld loads (27–29, 9). These observations suggest that we have identified the kinematic profile of a primitive unit action during unloaded movements. This temporal motor primitive may be analogous

**Posthypoxic-action myoclonus is a temporary form of myoclonus typically occurring after anesthetic accidents and myocardial infarction resulting in coma and severe global forebrain ischemia. See Weiner, W. J. & Lang, A. E. (1989) *Movement Disorders: A Comprehensive Survey* (Futura, Mount Kisco, NY).

to the visual primitives (edges, lines, etc.) recognized by the brain's visual processing system (30).

The fact that a common profile was identified from the movements of a pool of patients with a disparate size and severity of focal ischemic or hemorrhagic injuries to the cortex, subcortex, pons, and basal ganglia brain suggests that these structures do not generate the submovement shape. Although we cannot rule out the possibility that the residual function of these damaged structures is sufficient to generate submovement kinematics, our results imply that the primitive submovement emerges from deeper or distal structures in the nervous system, i.e., the remaining undamaged brain and brain stem, cerebellum, or spinal cord.

In conclusion, to our knowledge, our data provides strong, objective support for the conjecture made in the past by many other motor control researchers that a repertoire of movement primitives, each with a bell-shaped speed profile, constitute fundamental building blocks of complex motions. This precise mathematical characterization of submovement kinematics provides the key information to make it possible to deconvolve continuous movements objectively and reliably into their component submovements. That is, our result changes a "hard inverse problem" into a straightforward filtering problem and may contribute to a deeper understanding of the motor system, with important applications for neuroscience, neurorehabilitation, and robotics.

This work was supported in part by National Science Foundation Grant 8914032-BCS and the Burke Medical Research Institute.

1. Woodworth, R. S. (1899) Ph.D. thesis (Columbia University, New York).
2. Crossman, E. R. F. W. & Goodeve, J. (1983) *Q. J. Exp. Psychol.* **35,** 251–278.
3. Fitts, P. M. (1954) *J. Exp. Psychol.* **47,** 381–391.
4. Jagacinski, R. J., Hartzell, E. J., Ward, S. & Bishop, K. (1978) *J. Mot. Behav.* **10,** 123–131.
5. Jagacinski, R. J., Repperger, D. W., Moran, M. S., Ward, S. L. & Glass, B. (1980) *J. Exp. Psychol. Hum. Percept. Perform.* **6**, 309–320.
6. Morasso, P. & Mussa-Ivaldi, F. A. (1982) *Biol. Cybern.* **45,** 131–142.
7. Nelson, W. L. (1983) *Biol. Cybern.* **46,** 135–147.
8. Hogan, N. (1984) *J. Neurosci.* **4,** 2745–2754.
9. Hollerbach, J. M. & Atkeson, C. G. (1987) *J. Neurosci. Methods* **21,** 181–194.
10. Abend, W., Bizzi, E. & Morasso, P. (1982) *Brain* **105,** 331–348.
11. Flash, T. & Henis, E. (1994) *J. Cogn. Neurosci.* **3,** 220–230.
12. Milner, T. E. (1992) *Neuroscience* **49:2,** 487–496.
13. Von Hofsten, C. & Lindhagen, K. (1979) *J. Exp. Child Psychol.* **28,** 158–173.
14. Von Hofsten, C. (1979) *J. Hum. Mov. Stud.* **5,** 160–178.
15. Von Hofsten, C. (1980) *J. Exp. Child Psychol.* **30,** 369–382.
16. Lee, D., Port, N. L. & Georgopoulos, A. P. (1997) *Exp. Brain Res.* **116,** 421–433.
17. Berthier, N. E. (1996) *Dev. Psychol.* **32,** 811–823.
18. Meyer, D. E., Smith, J. E. K., Kornblum, S., Abrahms, R. A. & Wright, C. E. (1990) in *Attention and Performance: Motor Representation and Control*, ed. Jeannerod, M. (Lawrence Erlbaum, Hillsdale, NJ), Vol. 13.
19. Cybenko, G. (1989) *Math. Control Signal System* **2,** 303–314.
20. Hornik, K., Stinchcombe, M. & White, H. (1989) *Neural Networks* **2,** 359–366.
21. Poggio, T. & Girosi, F. (1990) *Science* **247,** 978–982.
22. Krebs, H. I. (1997) Ph.D. thesis (Massachusetts Institute of Technology, Cambridge, MA).
23. Aisen, M. L., Krebs, H. I., McDowell, F., Hogan, N. & Volpe, B. T. (1997) *Arch. Neurol.* **54,** 443–446.
24. Krebs, H. I., Hogan, N., Aisen, M. L. & Volpe B. T. (1998) *IEEE Trans. Rehab. Eng.* **6,** 75–87.
25. Hogan, N., Krebs, H. I., Sharon, A. & Charnnarong, J. (1995) U.S. Patent 5,466,213.
26. Pratt, J. W., Raiffa, H. & Schlaifer, R. (1995) *Statistical Decision Theory* (MIT Press, Cambridge, MA).
27. Morasso, P. (1981) *Exp. Brain Res.* **42,** 223–227.
28. Flash, T. & Hogan, N. (1985) *J. Neurosci.* **5,** 1688–1703.
29. Atkeson, C. G. & Hollerbach, J. M., (1985) *J. Neurosci.* **5**, 2318–2330.
30. Hubel, D. H. & Wiesel, T. N. (1979) *Sci. Am.* **241** (3), 150–162.